Physics Letters B 769 (2017) 166–170

Contents lists available at ScienceDirect

Physics Letters B

www.elsevier.com/locate/physletb

Unique prediction for high-energy J/ψ photoproduction: Color transparency and saturation

Dieter Schildknecht [a,b,*]

[a] Fakultät für Physik, Universität Bielefeld, D-33501 Bielefeld, Germany
[b] Max-Planck-Institut für Physik (Werner-Heisenberg-Institut), Föhringer Ring 6, D-80805 München, Germany

ARTICLE INFO

Article history:
Received 9 November 2016
Accepted 26 March 2017
Available online 30 March 2017
Editor: G.F. Giudice

Keywords:
Vector meson production
Deep inelastic scattering
Color transparency
Saturation

ABSTRACT

Based on the color-dipole picture, we present a successful parameter-free prediction for the recent high-energy J/ψ photoproduction data from the Large Hadron Collider. The experimental data provide empirical evidence for the transition from color transparency to saturation.

Inspired by experimental data [1] on J/ψ photoproduction, $\gamma p \to J/\psi\ p$, at very high energies obtained at the Large Hadron Collider (LHC), we revive our predictions [2,3] on J/ψ production based on the color-dipole picture (CDP).[1] As depicted in Figs. 1 and 2, the total photoabsorption cross section and the forward production of quark-antiquark states, $\gamma^* p \to (q\bar{q})^{J=1}_{T,L} p$, of total spin $J=1$ at low values of $x \cong Q^2/W^2 \ll 1$ are represented by [3,4]

$$\sigma_{\gamma^*_{T,L}p}(W^2, Q^2) = \int dz \int d^2r_\perp |\psi_{T,L}(r_\perp, z(1-z), Q^2)|^2 \times \sigma_{(q\bar{q})^{J=1}_{T,L}p}(\vec{r}_\perp\sqrt{z(1-z)}, W^2) \quad (1)$$

and

$$\left.\frac{d\sigma_{\gamma^*_{T,L}p\to(q\bar{q})^{J=1}_{T,L}p}}{dt}(W^2, Q^2)\right|_{t=0} = \frac{1}{16\pi}\int dz \int d^2r_\perp \left|\psi_{T,L}(r_\perp, z(1-z), Q^2)\right|^2 \times \sigma^2_{(q\bar{q})^{J=1}_{T,L}p}(\vec{r}_\perp\sqrt{z(1-z)}, W^2). \quad (2)$$

In standard notation, $|\psi_{T,L}(r_\perp, z(1-z), Q^2)|^2$ denotes the probability for the photon of virtuality Q^2 to couple to a $(q\bar{q})^{J=1}_{T,L}$ state specified by the transverse size $\vec{r}_\perp$ and the longitudinal momentum partition $0 \le z \le 1$, and $\sigma_{(q\bar{q})^{J=1}_{T,L}p}(\vec{r}_\perp\sqrt{z(1-z)}, W^2)$ denotes the $(q\bar{q})$-dipole-proton cross section at the total $\gamma^* p$ center-of-mass energy W. The two-gluon coupling of the $q\bar{q}$ dipole state requires a representation of the $(q\bar{q})$-color-dipole cross section of the form [3,4]

$$\sigma_{(q\bar{q})^{J=1}_{T,L}p}(\vec{r}_\perp\sqrt{z(1-z)}, W^2) = \int d^2l'_\perp \tilde{\sigma}_{(q\bar{q})^{J=1}_{T,L}p}(\vec{l}'^2_\perp, W^2)(1 - e^{-i\vec{l}'_\perp\cdot\vec{r}_\perp\sqrt{z(1-z)}}). \quad (3)$$

Upon introducing the mass, M, of the $(q\bar{q})^{J=1}$ states, and upon applying the optical theorem to relate $(q\bar{q})^{J=1}p$ forward scattering to the $(q\bar{q})^{J=1}p$ total cross section, we identically reformulate the total photoabsorption cross section (1) in terms of the $(q\bar{q})p$ forward-production cross section (2), obtaining [5][2]

$$\sigma_{\gamma^*_T p}(W^2, Q^2) = \sqrt{16\pi}\sqrt{\frac{\alpha R_{e^+e^-}}{3\pi}}\int\limits_{m_0^2} dM^2 \frac{M}{Q^2+M^2} \times \sqrt{\left.\frac{d\sigma_{\gamma^*_T p\to(q\bar{q})^{J=1}_T p}}{dt dM^2}\right|_{t=0}} \quad (4)$$

* Correspondence to: Fakultät für Physik, Universität Bielefeld, D-33501 Bielefeld, Germany
E-mail address: schild@physik.uni-bielefeld.de.

[1] Compare ref. [4] and the list of literature on the CDP quoted there.

[2] A correction related to the contributions due to a (small) real part of the $q\bar{q}$ forward-production amplitude is ignored in (4) and (5).

http://dx.doi.org/10.1016/j.physletb.2017.03.056

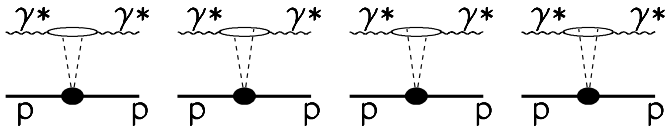

Fig. 1. The forward Compton amplitude.

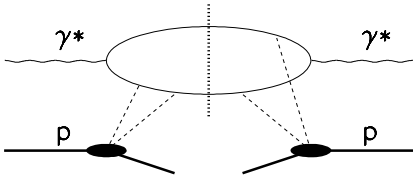

Fig. 2. One of the 16 diagrams for diffractive production. The vertical line indicates the unitarity cut corresponding to the diffractively produced final states, $(q\bar{q})^J$. Production of (discrete or continuum) vector states corresponds to $(q\bar{q})^J$ production with $J=1$.

and

$$\sigma_{\gamma_L^* p}(W^2, Q^2) = \sqrt{16\pi}\sqrt{\frac{\alpha R_{e^+e^-}}{3\pi}}\int_{m_0^2} dM^2 \frac{\sqrt{Q^2}}{Q^2+M^2} \times \sqrt{\left.\frac{d\sigma_{\gamma_L^* p\to(q\bar{q})_L^{J=1}p}}{dtdM^2}\right|_{t=0}}. \quad (5)$$

The representations (4) and (5) explicitly relate the transverse and longitudinal total photoabsorption cross sections to the diffractive forward-production cross sections,

$$\left.\frac{d\sigma_{\gamma_{T,L}^* p\to(q\bar{q})_{T,L}^{J=1}p}}{dtdM^2}\right|_{t=0} = \left.\frac{d\sigma_{\gamma_{T,L}^* p\to(q\bar{q})_{T,L}^{J=1}p}}{dtdM^2}(W^2, Q^2, M^2)\right|_{t=0}, \quad (6)$$

of a continuum of $(q\bar{q})^{J=1}$ states of mass M. The lower limit m_0^2 in (4) and (5), via quark-hadron duality,[3] for the (dominant) contribution due to light quarks fulfills $m_0 < m_\rho$, where m_ρ is the ρ-meson mass, and $R_{e^+e^-} = 3\sum_q Q_q^2$, where the sum runs over the actively contributing quark flavors, and Q_q denotes the quark charge.

The representations (4) and (5) for the photoabsorption cross section explicitly demonstrate that low-x photoabsorption is due to the coupling of the photon to $(q\bar{q})^{J=1}$ (vector) dipole states that subsequently propagate and interact via coupling to two gluons with the gluon field in the nucleon. The massive $q\bar{q}$ continuum contains the low-lying vector mesons, $\rho^0, \omega, \phi, J/\psi, \Upsilon$ etc. followed by more massive $J=1$ true continuum states, $X_{q\bar{q}}^{J=1}$, also diffractively produced via $\gamma^* p \to X_{(q\bar{q})}^{J=1} p$. For an appropriate magnitude of the kinematic variables, the $X_{(q\bar{q})}^{J=1}$ states appear as two-jet states with angular distribution characteristic for spin $J=1$.

For quantitative predictions, $\bar{\sigma}_{(q\bar{q})_{T,L}^{J=1}p}(\vec{l}_\perp'^2, W^2)$ in (3) must be specified. Agreement with experiment for the total photoabsorption cross section in (1), and, equivalently, in (4) and (5), then determines the diffractive (forward) production of vector states and allows for a parameter-free prediction of their photoproduction cross section (6). Indeed, for vector-meson production, specifically for J/ψ production,[4] we have [2,3]

$$\frac{d\sigma_{\gamma^* p\to J/\psi\, p}}{dt}(W^2, Q^2)\,|_{t=0} = \int_{\Delta M_{J/\psi}^2} dM^2 \int_{z_-}^{z_+} dz \frac{d\sigma_{\gamma^* p\to(c\bar{c})^{J=1}p}}{dt\, dM^2\, dz}(W^2, Q^2, z, m_c^2, M^2), \quad (7)$$

where

$$z_\pm = \frac{1}{2} \pm \frac{1}{2}\sqrt{1-4\frac{m_c^2}{M^2}}. \quad (8)$$

In (7), m_c denotes the mass of the charm quark, and $M^2 \equiv M_{c\bar{c}}^2$ denotes the mass squared of the $c\bar{c}$ state in the interval $\Delta M_{J/\psi}^2$ determined by the level spacing of the $c\bar{c}$ bound-state spectrum of states observed in e^+e^- annihilation.

Replacing the cross section for the open-charm continuum on the right-hand side in (7) by the cross section for $c\bar{c}$ production at threshold,

$$\frac{d\sigma_{\gamma^* p\to(c\bar{c})^{J=1}p}}{dt\, dM^2 dz}(W^2, Q^2, z, m_c^2, M^2) \longrightarrow \frac{d\sigma}{dt\, dM^2\, dz}\left(W^2, Q^2, z=\frac{1}{2}, M^2 = 4m_c^2 = M_{J/\psi}^2\right), \quad (9)$$

the integration in (7) simplifies to become [3]

$$\int_{4m_c^2}^{4m_c^2+\Delta M_{J/\psi}^2} dM^2 \int_{z_-}^{z_+} dz = \int_{4m_c^2}^{4m_c^2+\Delta M_{J/\psi}^2} dM^2 \sqrt{1-\frac{4m_c^2}{M^2}} \equiv \Delta F^2(m_c^2, \Delta M_{J/\psi}^2), \quad (10)$$

where

$$\Delta F^2(m_c^2, \Delta M_{J/\psi}^2) \equiv \int_{4m_c^2}^{4m_c^2+\Delta M_{J/\psi}^2} dM^2 \sqrt{1-\frac{4m_c^2}{M^2}} \int_0^1 dy = (4m_c^2 + \Delta M_{J/\psi}^2)\sqrt{\frac{\Delta M_{J/\psi}^2}{4m_c^2+\Delta M_{J/\psi}^2}} + 2m_c^2 \ln\frac{1-\sqrt{\frac{\Delta M_{J/\psi}^2}{4m_c^2+\Delta M_{J/\psi}^2}}}{1+\sqrt{\frac{\Delta M_{J/\psi}^2}{4m_c^2+\Delta M_{J/\psi}^2}}}. \quad (11)$$

With (9) to (11), the cross section (7) becomes

$$\left.\frac{d\sigma_{\gamma^* p\to J/\psi p}}{dt}(W^2, Q^2)\right|_{t=0} \longrightarrow \frac{d\sigma}{dt\, dM^2\, dz}\left(W^2, Q^2, z=\frac{1}{2}, M^2 = 4m_c^2 = M_{J/\psi}^2\right) \times \Delta F^2(m_c^2, \Delta M_{J/\psi}^2). \quad (12)$$

The cross section for J/ψ electroproduction in (12) is accordingly represented by charm-quark pair production at threshold multiplied by the factor $\Delta F^2(m_c^2, \Delta M_{J/\psi}^2)$ of dimension $\Delta M_{J/\psi}^2$.

In refs. [2,3] we have evaluated the J/ψ-production cross section (12) upon specifying the dipole cross section in (3) by the ansatz

$$\bar{\sigma}_{(q\bar{q})_T^{J=1}p}(\vec{l}_\perp'^2, W^2) = \bar{\sigma}_{(q\bar{q})_L^{J=1}p}(\vec{l}_\perp'^2, W^2) = \sigma^{(\infty)}(W^2)\frac{1}{\pi}\delta(\vec{l}_\perp'^2 - \Lambda_{sat}^2(W^2)), \quad (13)$$

[3] Massless quarks are used in the derivation of (4) and (5).

[4] The generalization to Υ-production is straight forward.

previously employed [4] in our (successful) representation of the body of experimental data on the total photoabsorption cross section (1), or equivalently, (4) and (5). The (asymptotic) dipole cross section $\sigma^{(\infty)}(W^2)$ depends logarithmically on W^2. The specification of $\sigma^{(\infty)}(W^2)$ and of the "saturation scale" $\Lambda^2_{sat}(W^2)$ will be given below.

With (13), one finds that the cross section (12) takes the simple explicit form [2]

$$\frac{d\sigma_{\gamma^* p\to J/\psi\ p}}{dt}(W^2, Q^2)\,\big|_{t=t_{\min}\cong 0} = \frac{3}{2}\frac{1}{16\pi}\frac{\alpha\, R^{(J/\psi)}}{3\pi}\left(\sigma^{(\infty)}(W^2)\right)^2\frac{\Lambda^4_{sat}(W^2)}{(Q^2+M^2_{J/\psi})^3} \times \frac{1}{\left(1+\frac{\Lambda^2_{sat}(W^2)}{Q^2+M^2_{J/\psi}}\right)^2}\Delta F^2(m_c^2, \Delta M^2_{J/\psi}), \tag{14}$$

where $R^{(J/\psi)} = \frac{4}{3}$.

We stress again that (14) provides a parameter-free prediction for J/ψ photo- and electroproduction, once the dipole cross section, $\sigma^{(\infty)}(W^2)$, and the saturation scale, $\Lambda^2_{sat}(W^2)$, in (13) are specified from agreement with experiment of the CDP prediction for the total photoabsorption cross section $\sigma_{\gamma^* p}(W^2, Q^2)$ in (1). The total J/ψ production cross section is obtained from (14) by multiplication [2] with the inverse of the experimentally known slope parameter of the J/ψ production diffraction peak.

In refs. [2,3] we compared the threshold-approximation result (14) with the (numerical) results obtained without relying on the threshold approximation (9). We found that (14), upon multiplication by an overall factor of magnitude 2/3, corresponding to $3/2 \to 1$ in (14), is in good agreement with the results that do not rely on the threshold approximation (9). In addition, in ref. [2], the cross section in (14) was modified by the replacement of $\sigma^{(\infty)}(W^2)$ by $\sigma'^{(\infty)}(W^2) = const\ \sigma^{(\infty)}(W^2)$, where the constant factor takes care of a so-called "skewing correction" and a correction for a small real part in the J/ψ production amplitude. The agreement with the ZEUS experimental data [6] for the Q^2 and the W dependence of J/ψ production was elaborated upon in detail in ref. [2].

In the present note, we concentrate on photoproduction, $Q^2 = 0$, and in particular we concentrate on the experimental results on the high-energy dependence of $\sigma_{\gamma p\to J/\psi p}(W)$, for $W \gtrsim 100$ GeV, recently presented by the LHCb collaboration [1]. The experimental data are reproduced in Fig. 3, taken from ref. [1]. At the energy of $W = W_1 = 100$ GeV, the LHCb result of $\sigma_{\gamma p\to J/\psi p}(W = W_1 = 100\ \text{GeV}) \cong 80$ nb is consistent with our theoretical prediction [2] and with the ZEUS experimental results [6]. With respect to the LHCb results in Fig. 3, we can accordingly restrict ourselves to an analysis of the energy variation of the measured cross section relative to the cross section at $W = W_1 = 100$ GeV. From (14), at $Q^2 = 0$, for $\sigma_{\gamma p\to J/\psi p}(W^2)$ in terms of $\sigma_{\gamma p\to J/\psi p}(W_1^2)$, we find

$$\sigma_{\gamma p\to J/\psi p}(W^2) = \frac{\left(1+\frac{M^2_{J/\psi}}{\Lambda^2_{sat}(W_1^2)}\right)^2}{\left(1+\frac{M^2_{J/\psi}}{\Lambda^2_{sat}(W^2)}\right)^2} \times \frac{\left(\sigma^{(\infty)}(W^2)\right)^2}{\left(\sigma^{(\infty)}(W_1^2)\right)^2}\sigma_{\gamma p\to J/\psi p}(W_1^2 = (100\ \text{GeV})^2), \equiv F_A(\Lambda^2_{sat}(W^2))F_B(W^2)\sigma_{\gamma p\to J/\psi p}(W_1^2 = (100\ \text{GeV})^2), \tag{15}$$

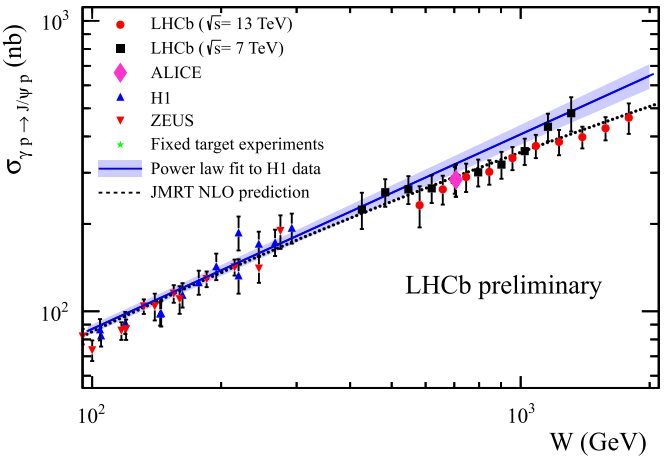

Fig. 3. The experimental results [1] from the LHCb collaboration. The figure is taken from ref. [1]. The theoretical results from the CDP (compare (14) as well as (15)) given in the last column of Table 1, are seen to agree with the experimental results from the LHCb collaboration.

where $\sigma_{\gamma p\to J/\psi p}(W_1^2 = (100\ \text{GeV})^2) = 80$ nb is to be inserted on the right-hand side in (15).

The dominant energy dependence of J/ψ photoproduction is due to the first factor, $F_A(\Lambda^2_{sat}(W^2))$, on the right-hand side in (15). Inserting $M_{J/\psi} = 3.1$ GeV, and [2]

$$\Lambda^2_{sat}(W^2) = B'\left(\frac{W^2}{1\ \text{GeV}^2}\right)^{C_2}, \tag{16}$$

where

$$B' = 0.340\ \text{GeV}^2, \quad C_2 = 0.276, \tag{17}$$

we find the results for $F_A(\Lambda^2_{sat}(W^2))$ shown in the fourth column of Table 1.

Concerning the magnitude of $F_B(W^2)$ in (15), we note that the (logarithmic) variation of $\sigma^{(\infty)}(W^2)$ with energy in the CDP is determined [4] by consistency of the $Q^2 \to 0$ limit of the total cross section $\sigma_{\gamma^* p}(W^2, Q^2)$ with the experimental results on photoproduction, $\sigma_{\gamma p}(W^2)$. The photoproduction limit in the CDP is given by [4]

$$\sigma_{\gamma p}(W^2) = \frac{\alpha R_{e^+e^-}}{3\pi}\sigma^{(\infty)}(W^2)\ln\frac{\Lambda^2_{sat}(W^2)}{m_0^2}, \tag{18}$$

where $m_0^2 = 0.15$ GeV^2. For $\sigma_{\gamma p}(W^2) \sim (\ln W^2)^2$, the dipole cross section $\sigma^{(\infty)}(W^2)$ increases as a single power of $\ln W$. According to (18) for $F_B(W^2)$ in (15), we have

$$F_B(W^2) \equiv \left(\frac{\sigma^{(\infty)}(W^2)}{\sigma^{(\infty)}(W_1^2)}\right)^2 = \left(\frac{\ln\frac{\Lambda^2_{sat}(W_1^2)}{m_0^2}}{\ln\frac{\Lambda^2_{sat}(W^2)}{m_0^2}}\right)^2\left(\frac{\sigma_{\gamma p}(W^2)}{\sigma_{\gamma p}(W_1^2)}\right)^2 \tag{19}$$

We adopt a simple asymptotic Pomeron dependence for photoproduction, $\sigma_{\gamma p} \simeq (W^2)^{0.08}$ [7], and from (19), we obtain the results for $F_B(W^2)$ given in the fifth column of Table 1.

Our results for the energy dependence of the J/ψ photoproduction cross section following from (14), according to (15) and (19), are presented in the last column of Table 1. A comparison to the experimental data in Fig. 3 shows agreement of our results from the CDP in Table 1 with the experimental results [1] from

Table 1
The results for $\sigma_{\gamma p\to J/\psi p}(W)$ in the CDP, compare (14). Explicitly, the results are based on (15) to (19).

W [GeV]	$\Lambda^2_{sat}(W^2)$ [GeV^2]	$\frac{M^2_{J/\psi}}{\Lambda^2_{sat}(W^2)}$	$F_A(\Lambda^2_{sat}(W^2))$	$F_B(W^2)$	$\sigma_{\gamma p\to J/\psi p}(W)$ [nb]
100	4.32	2.22	1	1	80
300	7.92	1.21	2.12	1.02	173
1000	15.4	0.624	3.93	1.11	349
2000	22.6	0.425	5.11	1.16	474

the LHCb collaboration. The failure of the power-law fit in Fig. 1 at large values of the energy W is an obvious consequence of the fact that in the CDP, due to the denominator in (14), the cross section is *not* proportional to the square of the saturation scale, $(\Lambda^2_{sat}(W^2))^2$. This behavior may be traced back to the different dependence on the dipole cross section in (1) and (2), respectively. For a discussion on the connection between $\Lambda^2_{sat}(W^2)$ and the gluon distribution in connection with J/ψ production, compare ref. [2]. As pointed out [2], the W dependence of $\Lambda^2_{sat}(W^2)\sim(Q^2/x)^{C_2}$ measured in $Q^2=0$ photoproduction (nevertheless) determines the x dependence of the gluon distribution function (gluon PDF) at sufficiently large values of $Q^2\gtrsim M^2_{J/\psi}$, even though the simple proportionality of the cross section to $\Lambda^4(W^2)$ and the square of the gluon distribution function does *not* hold in general.

In order to substantiate the interpretation of the experimental data, it will be useful to return from photoproduction to the general case of $Q^2\geq 0$ in (14). According to (14), concentrating on the W^2 dependence and suppressing a constant factor, we have

$$\begin{aligned}
&\frac{d\sigma_{\gamma^* p\to J/\psi p}(W^2,Q^2)}{dt}\Big|_{t\cong 0}\\
&\propto \frac{(\sigma^{(\infty)}(W^2))^2}{\left(1+\frac{Q^2+M^2_{J/\psi}}{\Lambda^2_{sat}(W^2)}\right)^2}\,\frac{\Delta F^2(m_c^2,\Delta M^2_{J/\psi})}{(Q^2+M^2_{J/\psi})}\\
&\cong\begin{cases}\dfrac{\Lambda^4_{sat}(W^2)(\sigma^{(\infty)}(W^2))^2}{(Q^2+M^2_{J/\psi})^2}\,\dfrac{\Delta F^2(m_c^2,\ \Delta M^2_{J/\psi})}{(Q^2+M^2_{J/\psi})},\\ \quad \text{for } \dfrac{Q^2+M^2_{J/\psi}}{\Lambda^2_{sat}(W^2)}\gg 1,\\ (\sigma^{(\infty)}(W^2))^2\,\dfrac{\Delta F^2(m_c^2,\Delta M^2_{J/\psi})}{(Q^2+M^2_{J/\psi})},\\ \quad \text{for } \dfrac{Q^2+M^2_{J/\psi}}{\Lambda^2_{sat}(W^2)}\ll 1.\end{cases}
\end{aligned}\tag{20}$$

The W dependence, according to (20), at any fixed value of $Q^2\geq 0$, is determined by either $\eta_{c\bar c}(W^2,Q^2)\gg 1$ or $\eta_{c\bar c}(W^2,Q^2)\ll 1$, respectively, where

$$\eta_{c\bar c}(W^2,Q^2)\equiv\frac{Q^2+M^2_{J/\psi}}{\Lambda^2_{sat}(W^2)}\tag{21}$$

generalizes the low-x scaling variable [4] of deep inelastic scattering (DIS),

$$\eta(W^2,Q^2)\equiv\frac{Q^2+m_0^2}{\Lambda^2_{sat}(W^2)}\tag{22}$$

to the case of heavy (charm) quarks. According to (20), in analogy to the total photoabsorption cross section, compare Fig. 4, we have either color transparency associated with $\eta_{c\bar c}(W^2,Q^2)\gg 1$ and $\sigma_{\gamma^* p\to J/\psi p}(W^2,Q^2)\sim\Lambda^4_{sat}(W^2)$, or else we have saturation, $\eta_{c\bar c}(W^2,Q^2)\ll 1$ and $\sigma_{\gamma^* p\to J/\psi p}\sim(\sigma^{(\infty)}(W^2))^2\sim(\ln W^2)^2$. The

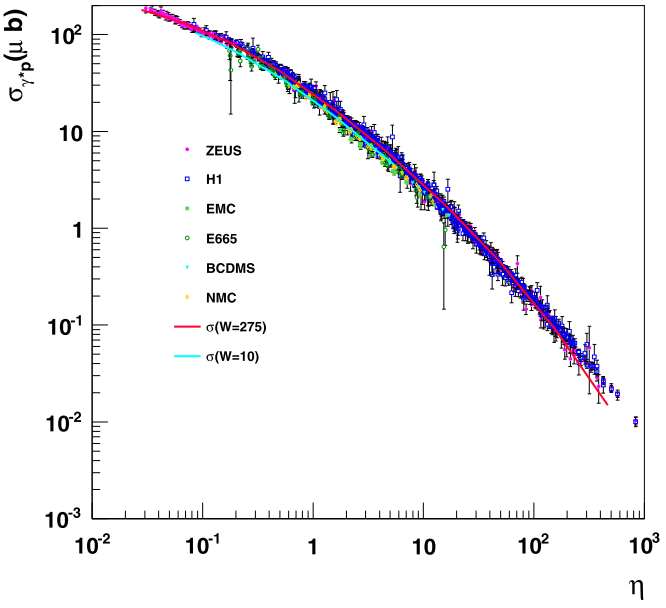

Fig. 4. The total photoabsorption cross section as a function of $\eta(W^2,Q^2)=(Q^2+m_0^2)/\Lambda^2_{sat}(W^2)$ (from ref. [4]).

conditions $\eta(W^2,Q^2)\gg 1$ and $\eta(W^2,Q^2)\ll 1$ for the case of the total photoabsorption cross section in Fig. 4, translate into $\eta_{c\bar c}(W^2,Q^2)\gg 1$ and $\eta_{c\bar c}(W^2,Q^2)\ll 1$, respectively.

We return to $Q^2=0$ photoproduction. In Table 1, third column, we see that for the energy range of the experimental data, the variable $\eta_{c\bar c}(W^2,Q^2=0)=M^2_{J/\psi}/\Lambda^2_{sat}(W^2)$ covers the range of

$$2.2\gtrsim\eta_{c\bar c}(W^2,Q^2)\geq 0.43.\tag{23}$$

This range corresponds to a region in the vicinity of $\eta_{c\bar c}(W^2,Q^2)=1$ that determines the transition from color transparency to saturation.[5] The (approximate) $\Lambda^4_{sat}(W^2)$ power law dependence, with increasing energy, breaks down to turn into a weak $(\ln W^2)^2$ dependence.

The deviation of the LHCb experimental data in Fig. 3 from the H1 power-law fit at $W\gtrsim 500$ GeV provides empirical evidence for the transition from color transparency to saturation. An extension [8] of a simple proportionality, $\Lambda^4_{sat}(W^2)\propto\left(\alpha_s(Q^2)xg(x,Q^2)\right)^2$, of the cross section of J/ψ production, $\sigma_{\gamma^* p\to J/\psi p}(W^2,Q^2)$, at fixed $Q^2\geq 0$ to large values of W does *not* lead to a decent high-energy behavior, such as $(\ln W^2)^2$, of the cross section in the true limit of $W\to\infty$ that is required to hold, however, and in fact is guaranteed by saturation as contained in the color-dipole picture.

[5] Our analysis leading to Table 1 was based on (14) or the first line in (20), or equivalently (15). The approximations in the second line of (20) in this connection must be considered as qualitative indications. They need a larger range in Q^2 and W^2 to become quantitatively reliable.

References

[1] LHCb-CONF-2016-007, August 22, 2016.
[2] M. Kuroda, D. Schildknecht, Phys. Lett. B 638 (2006) 473.
[3] M. Kuroda, D. Schildknecht, Eur. Phys. J. C 37 (2004) 205;
M. Kuroda, D. Schildknecht, Eur. Phys. J. C 44 (2005) 613, Erratum.
[4] M. Kuroda, D. Schildknecht, Phys. Rev. D 85 (2012) 094001;
D. Schildknecht, Mod. Phys. Lett. A 29 (2014) 1430028;
M. Kuroda, D. Schildknecht, Int. J. Mod. Phys. A 31 (2016) 1650157, arXiv:1606.07862 [hep-ph].
[5] M. Kuroda, D. Schildknecht, Phys. Rev. D 66 (2002) 094005;
M. Kuroda, D. Schildknecht, Phys. Rev. D 67 (2003) 094008.
[6] ZEUS Collaboration, S. Chekanov, et al., Eur. Phys. J. C 24 (2002) 345;
ZEUS Collaboration, S. Chekanov, et al., Nucl. Phys. B 695 (2004) 3.
[7] S. Donnachie, P. Landshoff, Phys. Lett. B 296 (1992) 227.
[8] S.P. Jones, et al., J. High Energy Phys. 11 (2013) 085, arXiv:1307.7099.